LANGMUIR

Article

Cite This: Langmuir XXXX, XXX, XXX-XXX

pubs.acs.org/Langmuir

Zwitterionic and Charged Lipids Form Remarkably Different Structures on Nanoscale Oil Droplets in Aqueous Solution

Yixing Chen, Halil I. Okur, Cornelis Lütgebaucks, and Sylvie Roke*

Laboratory for fundamental BioPhotonics (LBP), Institute of Bioengineering (IBI), and Institute of Materials Science (IMX), School of Engineering (STI), and Lausanne Centre for Ultrafast Science (LACUS), École Polytechnique Fédérale de Lausanne (EPFL), CH-1015 Lausanne, Switzerland

Supporting Information

ABSTRACT: The molecular structure of zwitterionic and charged monolayers on small oil droplets in aqueous solutions is determined using a combined second harmonic and sum frequency study. From the interfacial vibrational signature of the acyl chains and phosphate headgroups as well as the response of the hydrating water, we find that zwitterionic and charged lipids with identical acyl chains form remarkably different monolayers. Zwitterionic phospholipids form a closely packed monolayer with highly ordered acyl tails. In contrast, the charged phospholipids form a monolayer with a low number density and disordered acyl tails. The charged headgroups are oriented perpendicular to the monolayer rather than parallel, as is the case for zwitterionic lipids. These significant differences between the two types of phospholipids indicate important roles of phospholipid headgroups in the determination of properties of cellular membranes and lipid droplets. The observed behavior of charged phospholipids is different from expectations based on studies performed on extended planar interfaces, at which condensed monolayers are readily formed. The difference can be explained by nanoscale related changes in charge condensation behavior that has its origin in a different balance of interfacial intermolecular interactions.

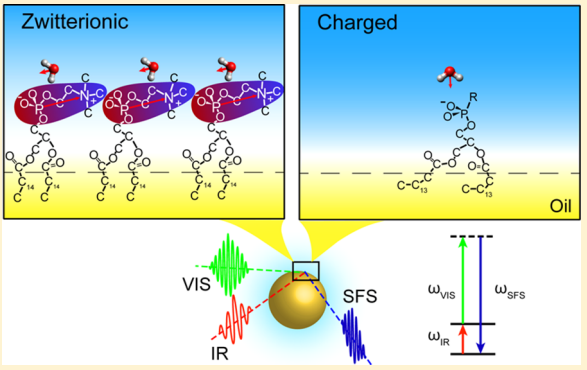

INTRODUCTION

Phospholipids are the building blocks of membranes and organelles in living cells.[1] Because of their excellent biocompatibility and intrinsic amphiphilicity, phospholipids are important pharmaceutical excipients in the delivery of highly lipophilic drugs, which compose a substantial fraction of the new drug candidates.[2,3] One important lipid-based delivery system consists of oral and injectable lipid emulsions, which are widely utilized and of increasing interest to the pharmaceutical industry.[3,4] In these lipid emulsions that have lipophilic drugs dissolved in the nanoscopic oil core, lipids serve as the emulsifier forming a monolayer at the oil/water interface and enhance the bioavailability of the delivered drugs. This lipid-monolayer-coated oil nanodroplet is similar to adiposomes (lipid droplet),[5] a naturally occurring organelle in cells.

The chemical functionality of these nanoscopic lipid monolayer systems and cellular membranes is expected to be largely determined by the chemical structure of the lipids and their interaction with the aqueous phase.[4,6] Zwitterionic phospholipids, such as phosphatidylcholine (PC) and phosphatidylethanolamine (PE), are the most abundant phospholipids in membranes and are mostly used in lipid emulsions for drug delivery.[3] Charged phospholipids such as phosphatidylserine (PS), phosphatidic acid (PA), and phosphatidylglycerol (PG) are often a secondary component in terms of abundance yet they play roles in cell signaling and stabilizing oil nanodroplets.[4,6,7] The molecular-level details of how phospholipids are structured at the oil/water interface and stabilize oil nanodroplets for lipid droplets and for efficient drug delivery are thus of great interest.[8,9] Different experimental techniques have been employed to study phospholipids using membrane model systems such as Langmuir monolayers and supported bilayers. X-ray[10−13] and neutron scattering[14−16] studies have elucidated the distance and position of phospholipids in Langmuir monolayers in different phases at the air/liquid interface and in planar-supported phospholipid bilayers. Fluorescence microscopy[17−19] is able to show phase segregation in Langmuir monolayers and substrate-supported bilayers and enables the study of the lateral structure of giant unilamellar vesicles by using fluorescent-dye-labeled phospholipids. Pressure−area isotherm measurements[20,21] explore the phase transition of Langmuir monolayers by examining the relation between the packing density of phospholipids and the applied lateral pressure. Sum frequency generation (SFG) is used extensively in studies of Langmuir monolayers at the air/water interface[22−29] and the liquid/liquid interface[30,31] as well

Special Issue: Early Career Authors in Fundamental Colloid and Interface Science

Received: August 16, 2017
Revised: October 6, 2017
Published: October 11, 2017

DOI: 10.1021/acs.langmuir.7b02896
Langmuir XXXX, XXX, XXX−XXX

as substrate-supported phospholipid monolayers[32,33] and bilayers[34−36] to probe molecular structures of phospholipids and water. Molecular dynamics (MD) simulations[37−40] of model membrane systems, including phospholipid monolayers, bilayers, and vesicles, provide some insight into the structure and properties of phospholipids as well as their interactions with ions. It is worth noting that in these studies relatively condensed monolayers with an average molecular area much smaller than 100 Å^2 are formed at planar interfaces.

In contrast to extended planar model membranes, direct probing of the molecular structure of lipid droplet systems with different types of phospholipids remains fairly elusive. Recent vibrational sum frequency scattering (SFS) studies have shown that it is possible to determine the molecular-level structure of PC lipid monolayers around hexadecane droplets, including DPPC[41] and lyso-PC.[42] This new membrane model system enables the study of the nanoscale interface as it really is and also has a number of advantages over the above-mentioned model systems. Compared to Langmuir monolayers or supported lipid membranes,[29,43−45] the oil nanodroplets contain an ∼1000-fold larger surface to volume ratio (in a small sample volume) and are easy to prepare. The 60 μL sample volume and ∼100 nm radius ensure that the influence of impurities is minimal and the in situ production of the droplets in aqueous solution limits oxidation from ambient air and possible substrate influences.[41,46] In addition to SFS, second harmonic scattering (SHS) can be used to probe the orientational ordering of water at droplet and liposome interfaces. This method was introduced by the Eisenthal laboratory in 1996 to probe the adsorption of malachite green dye on colloidal particles employing a fixed-angle forward-scattering detection scheme.[47] Liposomes were also probed with the same method.[48,49] More recently, angle-resolved polarimetric second harmonic scattering was used as a means to detect the orientational order of water at droplet and liposome interfaces.[50−53] The aqueous response was related to the charge asymmetry of interface hydration[54] and the distribution of oriented water and ions in the Stern layer.[50,53]

Here, we investigate the molecular-level structure of five phospholipids with different headgroups but identical acyl chains: 1,2-dipalmitoyl-*sn*-glycero-3-phosphocholine (DPPC), 1,2-dipalmitoyl-*sn*-glycero-3-phosphoethanolamine (DPPE), 1,2-dipalmitoyl-*sn*-glycero-3-phospho-L-serine (DPPS), 1,2-dipalmitoyl-*sn*-glycero-3-phospho-(1′-*rac*-glycerol) (DPPG), and 1,2-dipalmitoyl-*sn*-glycero-3-phosphate (DPPA). The first two, DPPC and DPPE, are zwitterionic, and the others are anionic under pH-neutral conditions. (See Figure S1 for the chemical structures.) We chose these lipids in order to investigate the effects of charge and intermolecular interactions between lipid headgroups on the formation of lipid monolayers on nanoscale (100 nm) droplets. It was recently shown that nanoscale interfacial systems behave very differently compared to extended planar interfaces of the same composition.[51,55,56] One can ask if for membranes similar effects can be expected. We find that intermolecular interactions between the phospholipid headgroups result in remarkably different structures for charged and zwitterionic lipids around small oil droplets in water. Zwitterionic phospholipids form packed liquid condensed (LC) phaselike monolayers with all-trans acyl chains that are almost perpendicular to the monolayer plane (i.e., the surface of the nanodroplet). The headgroup of zwitterionic phospholipids is oriented almost parallel to the monolayer plane. Intermolecular interactions between headgroups orient interfacial water dipoles parallel to the monolayer plane. In contrast, anionic phospholipids form sparse monolayers with highly disordered acyl chains. The anionic phospholipid headgroup is oriented perpendicular to the monolayer plane to maximize hydrogen bonding and electrostatic interactions with water. The electrostatic field from the net charge of the headgroup leads to water ordering observed as an increase in the SHS intensity. These significant differences in the packing and interfacial structure between zwitterionic and charged phospholipids compared to that at planar interfaces arise from a different balance of intermolecular interactions.

MATERIALS AND METHODS

Materials. Hexadecane ($C_{16}H_{34}$, 99.8%, Sigma-Aldrich), d_{34}-hexadecane ($C_{16}D_{34}$, 98% d, Cambridge Isotope), 1,2-dipalmitoyl-*sn*-glycero-3-phosphocholine (DPPC, 99%, Avanti), 1,2-dipalmitoyl-*sn*-glycero-3-phosphoethanolamine (DPPE, 99%, Avanti), 1,2-dipalmitoyl-*sn*-glycero-3-phospho-L-serine (DPPS, 99%, Avanti), 1,2-dipalmitoyl-*sn*-glycero-3-phospho-(1′-*rac*-glycerol) (DPPG, 99%, Avanti), and 1,2-dipalmitoyl-*sn*-glycero-3-phosphate (DPPA, 99%, Avanti) were used as received. All aqueous solutions were made with ultrapure water (H_2O, Milli-Q UF plus, Millipore, Inc., electrical resistance of 18.2 MΩ cm; D_2O, 99.8%, Armar, >2 MΩ cm). Glassware was cleaned with a 1:3 H_2O_2/H_2SO_4 solution, after which it was thoroughly rinsed with ultrapure water (H_2O, Milli-Q UF plus, Millipore, Inc., electrical resistance of 18.2 MΩ cm).

Three-Dimensional Monolayers on Oil Nanodroplets. In water, these were prepared with 2 vol % d_{34}-hexadecane (hexadecane) in D_2O (H_2O) for SFS (for SHS). We mixed the solutions with lipid powders to reach a lipid concentration of 1 mM at a temperature of at least 5 °C above the transition temperature of the phospholipid by using a hand-held homogenizer (TH, OMNI International) for 4 min and an ultrasonic bath (35 kHz, 400 W, Bandelin) for the same duration. The resultant droplet system was used for SFS measurements and was diluted to 0.1 vol % hexadecane with pure water for SHS measurements. The size distribution of the nanodroplets was measured with dynamic light scattering (Malvern ZS nanosizer). The nanodroplets had a mean hydrodynamic radius in the range of 75−120 nm with a polydispersity index (PDI) of less than 0.3. The hydrodynamic radii were calculated from the intensity autocorrelation function using the optical properties of the liquids (d_{34}-hexadecane, hexadecane, H_2O, and D_2O). Although the prepared nanoemulsions are stable for at least several weeks, all samples were freshly prepared before each measurement. The samples were stored and measured in sealed cuvettes. All measurements were performed at 24 °C. The whole procedure from sample preparation to actual measurement took place in a time frame of no more than a few days.

Second Harmonic Scattering. These measurements were performed using the same SHS setup as previously described in ref 57. Briefly, 200 kHz 190 fs laser pulses with a pulse energy of 0.25 μJ (incident laser power P = 50 mW) and a center wavelength of 1028 nm were focused into a cylindrical glass sample cell (4.2 mm inner diameter, high-precision cylindrical glass cuvettes, LS Instruments). The polarization of the input pulses was controlled by a Glan-Taylor polarizer (GT10-B, Thorlabs) and a zero-order half-wave plate (WPH05M-1030). A long-pass filter (FEL0750, Thorlabs) was placed before the sample to ensure that no other frequencies except that of the laser pulse would interact with the sample. The beam waist of the focused pulses had a diameter of ∼35 μm and a corresponding Rayleigh length of ∼0.94 mm. The scattered SH light was filtered (ET525/50, Chroma), polarized (GT10-A, Thorlabs), collected with a plano-convex lens (f = 5 cm), and finally focused into a gated PMT (H7421-40, Hamamatsu). The scattering pattern was recorded at a step of 5° with an acceptance angle of 3.4°. The plotted data represent the SH intensity corrected for the background hyper-Rayleigh scattering and were normalized to the SSS intensity of pure water:

DOI: 10.1021/acs.langmuir.7b02896
Langmuir XXXX, XXX, XXX−XXX

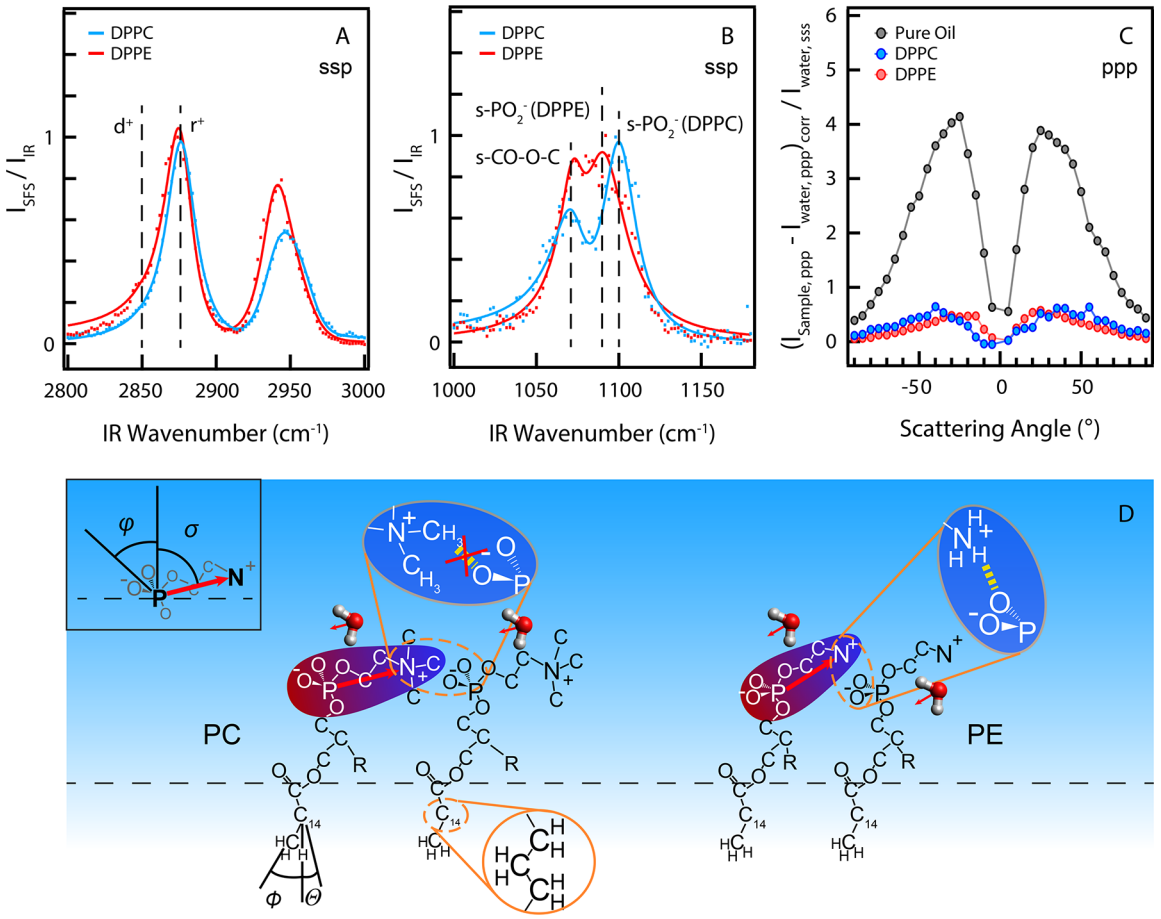

Figure 1. (A) Normalized SFS spectra in the C−H stretching region of DPPC and DPPE monolayers on 100-nm-radius d_{34}-hexadecane nanodroplets (2 vol %) in D_2O. The spectra are normalized to the s-CH_3 stretching mode (r^+). (B) Normalized SFS spectra in the P−O stretching region of the vibrational spectrum. The spectral fits (solid curves) in panels A and B are obtained using the procedure described in ref 64. (See S3 in the SI for more details.) The SFS spectra were recorded in the SSP polarization combination. This three-letter code for the polarization combination represents the polarization of each beam from high frequency to low frequency, with P(S) referring to light polarized parallel (perpendicular) to the scattering plane. (C) Normalized SHS patterns of oil nanodroplets with and without a zwitterionic phospholipid monolayer. The patterns have been corrected for intensity differences due to differences in the number density and size distribution of the nanodroplets, and the resulting scattered droplet intensity was then normalized to the intensity of bulk water measured in the SSS polarization combination (S6 in the SI of ref 65.) (D) Illustration of the interfacial structure of zwitterionic phospholipid monolayers on oil nanodroplets with an indication of the relevant angles. The big red arrow represents the P−N dipole of the phospholipid headgroup, and the small red arrows represent the water dipoles. −R represents the group of $-OCO(CH_2)_{14}CH_3$. Most of the H atoms are omitted for simplicity. The horizontal dashed line indicates the plane of the interface.

$$\frac{(I(\theta)_{SHS,droplets,PPP} - I(\theta)_{HRS,solution,PPP})_{corr}}{I(\theta)_{HRS,water,SSS}}$$

All data points were acquired with a 20 × 1 s acquisition time and a gate width of 10 ns. The reproducibility of the SHS measurements is in the range of 1−2%.

Vibrational Sum Frequency Scattering. The spectra were recorded using the same SFS setup as previously described in refs 58 and 50. Briefly, broadband infrared (IR) laser pulses centered at 2900 cm^{-1} (fwhm = 160 cm^{-1}) for the C−H stretching modes or 1090 cm^{-1} (fwhm = 123 cm^{-1}) for the P−O stretching modes and visible (vis) pulses at 800 nm (fwhm = 10 cm^{-1}) at a repetition rate of 1 kHz were focused and overlapped under an angle of 15° (as measured in air) in a sample cuvette with a path length of 200 μm. The scattered SF light was collimated at a scattering angle of 57° (as measured in air) with a plano-convex lens (f = 15 mm, Thorlabs LA1540-B) and passed through two short-pass filters (3rd Millenium, 3RD770SP). The SF light was spectrally dispersed with a monochromator (Acton, SpectraPro 2300i) and detected with an intensified CCD camera (Princeton Instruments, PI-Max3) using a gate width of 10 ns. The acquisition time for a single spectrum was set to 150 s for the C−H stretching region and 300 s for the P−O stretching region. The polarization of the SF, vis, and IR beams was controlled by a Glan-Taylor prism (Thorlabs, GT15-B), a half-wave plate (EKSMA, 460-4215) and a polarizing beam splitter cube (CVI, PBS-800-050), and two BaF_2 wire grid polarizers (Thorlabs, WP25H-B), respectively. All shown SFS spectra were normalized by an SF spectrum obtained in reflection geometry from a z-cut quartz crystal for the C−H stretching region or from a gold mirror for the P−O stretching region.

RESULTS AND DISCUSSION

Zwitterionic (Neutral) Lipids. The 3D phospholipid monolayer system consists of a dispersion of ∼100-nm-radius phospholipid-coated hexadecane droplets that are prepared by sonicating a mixture of 1 mM phospholipid molecules and 2 vol % hexadecane in water. The molecular structure of the monolayers is determined by SFS and SHS. Coherent SFS and SHS rely on a second-order nonlinear optical process that is forbidden in isotropic media (such as most liquids).[59] Because the interfaces between isotropic media inherently possess a breaking of the spatial centrosymmetry in the direction normal to the surface, SFS and SHS are sensitive to

DOI: 10.1021/acs.langmuir.7b02896
Langmuir XXXX, XXX, XXX−XXX

structuring on molecular length scales at interfaces.[59] The SFS measurements are used to probe interfacial C−H and P−O stretching modes of the phospholipids. By selectively deuterating the oil phase, the vibrational spectrum of the C−H region reports on the acyl chain conformation of the phospholipids. The amplitude ratio of the symmetric methylene (d^+) and the symmetric methyl (r^+) stretching modes, referred to as the d^+/r^+ ratio, is an empirical indicator of chain order.[60−62] A value of $d^+/r^+ \ll 1$ is associated with a stretched all-trans acyl chain conformation, whereas a value of $d^+/r^+ > 1$ indicates that gauche defects dominate the measured vibrational spectrum. Furthermore, the orientation of the acyl chains in the LC phase can be determined from the amplitude ratios of the symmetric and antisymmetric stretching modes in the SFS spectrum.[41] The orientation of the PO_2^- group in the lipid headgroup can be determined by analyzing the amplitude of the symmetric PO_2^- stretching mode in the SFS spectra in the SSP and PPP polarization combinations.[63] The angle-resolved SHS measurements report on the orientational order of all dipolar (and thus water) molecules at the interface in the direction of the interfacial normal.[51,52]

Figure 1 shows normalized SFS spectra of the acyl tail and headgroup regions of DPPC (blue curve) and DPPE (red curve) monolayers on d_{34}-hexadecane oil nanodroplets in D_2O. The C−H stretching (2800−3000 cm^{-1}, 1A) and P−O stretching (1000−1200 cm^{-1}, 1B) regions of the vibrational spectrum were both probed. The DPPC and DPPE SFS spectra in Figure 1A clearly show several modes:[22,30,35,66] the symmetric (s)-CH_3 stretch (~2876 cm^{-1}, r^+) and the antisymmetric (as)-CH_3 stretch (~2965 cm^{-1}, r^-) along with the s-CH_3 Fermi resonance (~2933 cm^{-1}, r^+_{FR}). The s-CH_2 stretching mode (d^+) at ~2852 cm^{-1} is visible in the DPPE spectrum, but it is very weak. As discussed in detail in ref 41 for DPPC, these spectra, with their typical low intensity of the d^+ mode and high intensity of the r^+ mode ($d^+/r^+ \rightarrow 0$), originate from acyl chains that have a conformation that is very close to all-trans. As determined previously, the structure of the DPPC monolayer resembles the LC phase in which the lipids have a projected area of 48 $Å^2$/phospholipid.[41] The spectrum of DPPE monolayers is very similar to that of DPPC, with $d^+/r^+ \sim 0.0$, indicating that the monolayers are also in the LC state. The average tilt angle of the acyl chains ($\langle\Theta\rangle$) and CH_3 groups ($\langle\phi\rangle$) of DPPC and DPPE with respect to the surface normal (illustrated in Figure 1D) can be estimated by assuming a certain orientational distribution function of the molecular groups. Assuming a δ function, which seems reasonable given the highly ordered acyl tails with the all-trans conformation, the average tilt angle of the CH_3 group is $\langle\phi\rangle = 40 \pm 4°$ for DPPC and $\langle\phi\rangle = 41 \pm 4°$ for DPPE. Because $\langle\Theta\rangle = |41.5 - \langle\phi\rangle|$,[22] we have $\langle\Theta\rangle = 2 \pm 4°$ for DPPC and $\langle\Theta\rangle = 1 \pm 4°$ for DPPE for the relative angle of the acyl chains with respect to the surface normal. Thus, these DPPC and DPPE monolayers have their acyl chains oriented normal to the interface in the LC phase. Previous X-ray diffraction measurements have reported a tilt angle of $\langle\Theta\rangle = 0°$ for DPPC monolayers in the LC phase at the air/water interface in contact with an ultrathin oil film[13] and $\langle\Theta\rangle$ of almost 0° for DLPE and 12° for DMPC in single crystals,[67] close to the ones found here. SFG studies of DPPC monolayers[22,24,29,31] and DPPE monolayers[68] at high packing densities show similar structures.

Figure 1B shows two peaks in the P−O stretching region for DPPC and DPPE monolayers: a peak at ~1073 cm^{-1}, assigned to the ester s-CO−O−C stretching mode, and a peak at ~1100 cm^{-1} (for DPPC) or ~1090 cm^{-1} (for DPPE) assigned to the s-PO_2^- stretching mode.[24,32] The resonance frequency of the s-PO_2^- stretching mode is very sensitive to intermolecular interactions, such as the hydration environment or headgroup−headgroup interactions.[24,69] DPPS-DOPC mixed liposomes in water display a red shift in the s-PO_2^- stretching mode, which was attributed to intermolecular $PO_2^-\cdots NH_3^+$ bond formation between lipid headgroups.[63] Counter ion (e.g., Ca^{2+} or Na^+)-induced dehydration of lipid headgroups leads to a blue shift in the s-PO_2^- stretching mode of DPPC monolayers in the Langmuir trough.[70,71] When such DPPC monolayers expand from the tightly packed LC phase to the LE phase, the s-PO_2^- stretching mode displays a red shift of ~10 cm^{-1}, indicating that some electron clouds of the PO_2^- bond are shared with adjacent water molecules to form H-bonds.[24] For DPPE, only a subtle shift of ~2 cm^{-1} was reported in a surface-pressure isotherm study when the DPPE Langmuir monolayer expands.[68] On the other hand, the influence of intermolecular interactions on the monolayer packing between these two phospholipids is also reflected in the significant difference in the transition temperature of the corresponding lipid bilayers: 41 °C for DPPC and 63 °C for DPPE.[72] Given the higher phase transition temperature of DPPE compared to that of DPPC, which is attributed to intermolecular H-bonding between lipid headgroups, it can be expected that a similar red shift will occur for DPPE monolayers compared to DPPC monolayers. Thus, it is likely that the observed 10 cm^{-1} red shift of the s-PO_2^- stretching mode in the SFS spectrum of Figure 1B indicates a stronger intermolecular interaction between DPPE headgroups in the monolayer compared to DPPC.

Analyzing the amplitude ratio of the s-PO_2^- stretching mode in different polarization combinations (see S3 and S5 in the SI and ref 63), we find an average tilt angle, $\langle\varphi\rangle$, of the PO_2^- headgroup with respect to the surface normal of 60 ± 3° and 66 ± 3° for DPPC and DPPE, respectively. For the ensemble orientation of the phospholipid headgroup, we use $\langle\sigma\rangle$ to represent the average tilt angle of the P (phosphorus atom)−N (nitrogen atom) vector of the phospholipid headgroup with respect to the surface normal. It can be observed that a smaller $\langle\varphi\rangle$ is related to a larger $\langle\sigma\rangle$: $\langle\varphi\rangle = 59°$ and $\langle\varphi\rangle = 64°$ have been reported for DPPC monolayers in the LC phase at the air/water interface and at the air/0.5 M NaCl solution interface, respectively, in an SFG study by Allen;[71] $\langle\sigma\rangle = 75.3°$ and $\langle\sigma\rangle = 66.2°$ have been reported for DPPC bilayers in water and in a 0.2 M NaCl solution, respectively, by MD simulations.[73] Similar differences have also been observed in MD simulations of DOPC bilayers between these two conditions.[74] Therefore, the observed larger tilt angle of $\langle\varphi\rangle = 66 \pm 3°$ for the PO_2^- headgroup for DPPE indicates a smaller tilt angle $\langle\sigma\rangle$ of the P−N dipole with respect to the surface normal than for DPPC. The smaller tilt angle of the P−N vector for DPPE suggests that DPPE forms a more tightly packed monolayer than does DPPC. Intermolecular $PO_2^-\cdots NH_3^+$ H-bonding combined with electrostatic interactions results in a stronger interaction between DPPE molecules than between DPPC molecules. This is in agreement with NMR studies performed on lipid pellets and surface pressure−area studies of lipid monolayers in circular troughs that report a "condensing" effect of the hydroxyl group in the headgroup of PE lipids.[75] The choline dipole of the PC lipids is found to be parallel to the membrane plane, and the hydroxyl group of the PE lipids alters the headgroup conformation of PE lipids to form a more condensed layer.[76]

DOI: 10.1021/acs.langmuir.7b02896
Langmuir XXXX, XXX, XXX−XXX

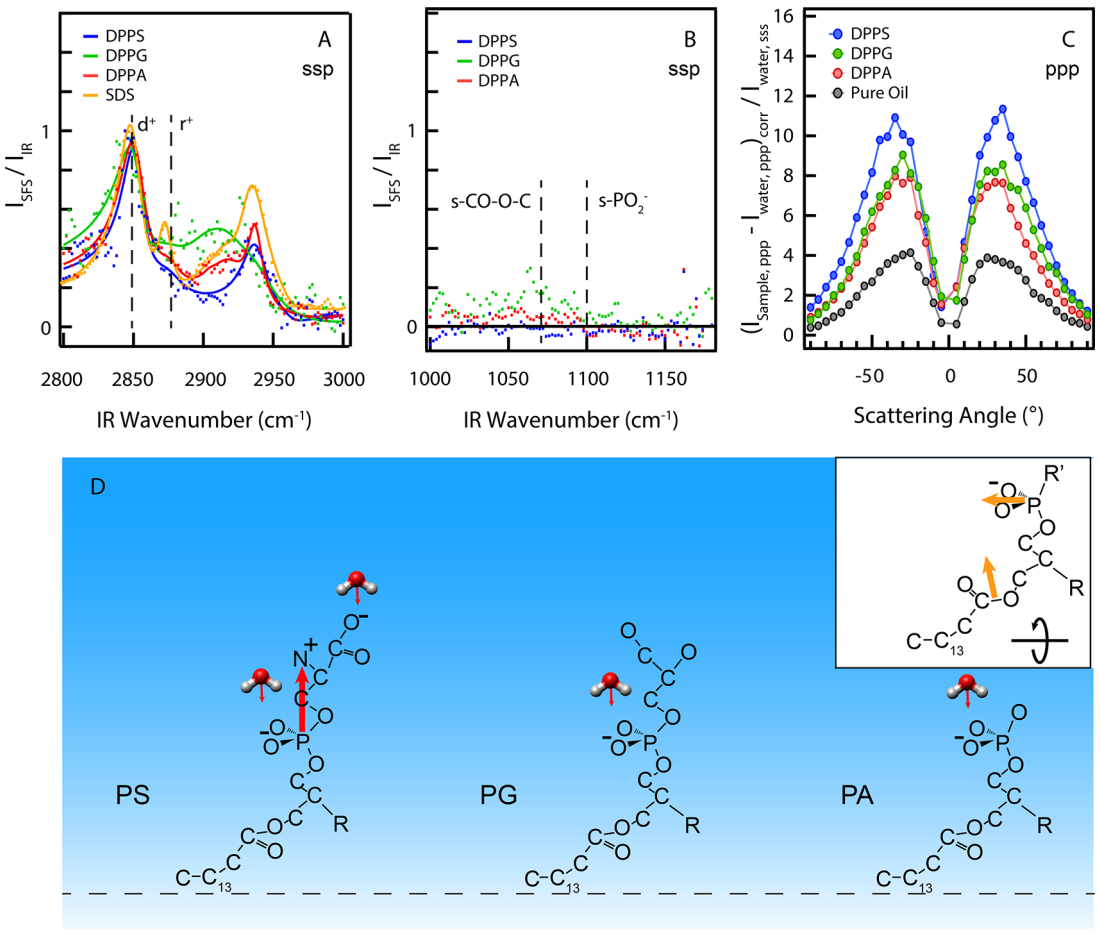

Figure 2. (A) Normalized SFS spectra of the DPPS (1 mM), DPPG (1 mM), DPPA (1 mM), and SDS (10 mM) monolayers on oil (d_{34}-hexadecane) nanodroplets (2 vol %) in D_2O for the C−H stretching modes. The spectra are normalized to the s-CH_2 stretching mode (r^+). The data of SDS is adapted from ref 51. (B) SFS spectra for the P−O stretching modes. The solid curves are respective spectral fits. (C) Normalized SHS patterns of oil nanodroplets with and without an anionic phospholipid monolayer. Differences in the number density and size of nanodroplets between different samples are corrected. (D) Illustration of the interfacial structure of anionic phospholipid monolayers on oil nanodroplets. The big red arrow represents the P−N dipole of the phospholipid headgroup, and the small red arrows represent the water dipoles. The orange arrows in the inset represent the vibrational dipoles of the s-PO_2^- and s-CO−O−C stretching modes. −R represents the group of $-OCO(CH_2)_{14}CH_3$, and −R′ represents the end headgroup of charged phospholipids. All of the H atoms are omitted for simplicity. The horizontal dashed line indicates the plane of the interface.

Figure 1C shows SHS patterns of the same phospholipid-monolayer-covered oil nanodroplets (blue for DPPC and red for DPPE), as in Figure 1A,B, as well as bare oil nanodroplets (black). The data was recorded in the PPP polarization combination, with all beams polarized parallel to the scattering plane, and was corrected for differences in the size distribution and droplet number density between measured samples (as described in ref 63). The intensity of a bulk solution that contained no droplets was subtracted from the measured intensities. The data was normalized to the SHS response of bulk water in the SSS polarization combination, which constitutes an isotropic scattering pattern. For bare oil nanodroplets, a significant population of water molecules have their H atoms pointing toward the interface[51,77] as a consequence of the negative surface charge (the origin of which is yet unexplained[78]). It can be seen that compared to the intensity of neat oil nanodroplets in H_2O, the SHS intensities of DPPC- and DPPE-coated nanodroplets are ∼8 times smaller. This means that the zwitterionic phospholipid monolayers significantly reduce the orientational order of water molecules along the surface normal.[51,79]

The close packing of the acyl tails, their average tilt angles, the loss in orientational order of the water molecules along the surface normal, and the average orientational angle of the P−N vector of the headgroup suggest that intermolecular interactions are present between the lipid headgroups of both types of zwitterionic phospholipids. Indeed, MD simulations of DMPC bilayer membranes have suggested that adjacent PC phospholipid molecules in a membrane interact by means of charge pairing between the PO_2^- and $N(CH_3)_3^+$ groups.[80,81] MD simulations[82,83] of DPPE bilayers and infrared vibrational spectroscopy studies[84] of microcrystalline DPPE dispersed in water have reported that the amine hydrogens of one PE group can H-bond to the phosphate group of an adjacent PE ($PO_2^-\cdots NH_3^+$). Thus, at the used concentration of phospholipids, the surface structures of the zwitterionic monolayers resemble what one would expect for a phospholipid monolayer in the LC phase of an extended planar interface. Previous studies of lipid monolayers on extended planar interfaces indicate that charged phospholipids also form condensed monolayers that are comparable to those of zwitterionic phospholipids.[32,85] We

DOI: 10.1021/acs.langmuir.7b02896
Langmuir XXXX, XXX, XXX−XXX

will now examine whether this is also the case for charged phospholipids on oil nanodroplets.

Charged Lipids. Figure 2 shows normalized SFS spectra of the acyl tail and headgroup regions of DPPS (blue curve), DPPG (green curve), and DPPA (red curve) monolayers on ∼100-nm-radius oil d_{34}-hexadecane nanodroplets in D_2O. Figure 2A,B shows the C−H and P−O stretching regions of the vibrational spectrum. The spectra of all charged phospholipids in both spectral regions are quite similar, but in comparison to the zwitterionic phospholipids (Figure 1), they are remarkably different. The vibrational modes that are apparent in the spectra of Figure 2A are the s-CH_2 stretch (∼2852 cm^{-1}, d^+), the as-CH_2 stretch (∼2919 cm^{-1}, d^-), and the s-CH_2 Fermi resonance (∼2905 cm^{-1}, d^+_{FR}). The (s)-CH_3 and (as)-CH_3 stretching modes at ∼2876 cm^{-1} (r^+) and ∼2965 cm^{-1} (r^-) are not clearly distinguishable. The d^+/r^+ ratios are 3.9 ± 0.2, 3.0 ± 0.2, and 4.3 ± 0.2 for DPPS, DPPG, and DPPA, respectively. It is interesting that the recorded C−H region spectra are almost indistinguishable from the SFS spectrum recorded from dilute sodium dodecyl sulfate (SDS) monolayers on hexadecane nanodroplets in D_2O (orange curve in Figure 2A, with d^+/r^+ = 3.7 ± 0.2)[51] The SDS monolayers were characterized in depth in refs 51, 55, and 64. It was found that DS^- is only sparsely populated at the surface of nanodroplets, in contrast to planar interfaces, and has its disordered acyl tail lying parallel to the interface. Given the high values for the d^+/r^+ ratio and the comparatively low overall SFS intensities of all charged phospholipids compared to that of zwitterionic phospholipids, it seems that the charged phospholipids have highly disordered acyl chains with many gauche defects and they do not form a densely packed monolayer. This also indicates that the headgroup orientation and environment of charged phospholipids could be different from that of the zwitterionic phospholipids.

Figure 2B shows the P−O stretching region spectra for the same samples. It can be seen that, within the signal-to-noise ratio of our system, there are no vibrational modes visible. The other polarization combinations (PPP and SPS) do not display any intensity (not shown). The vanishing SFS response implies that the vibrational dipoles of the s-PO_2^- and s-CO−O−C stretching modes are primarily oriented parallel to the droplets' interfacial plane. Such orientation renders these vibrational modes invisible to SFS because the interface likely has azimuthal symmetry.[59] Figure 2C shows the SHS patterns, recorded as described above, for the DPPS-, DPPG-, and DPPA-coated nanodroplets in H_2O with differences in the size distribution and droplet number density corrected. The SHS intensity of the anionic phospholipid monolayer-covered nanodroplets is more than 2 times higher than that of the neat oil nanodroplets. This significant increase in the SHS intensity indicates more orientational order of water along the surface normal. Because the DPPS, DPPG, and DPPA molecules are all charged under pH-neutral conditions, there is an electrostatic field emanating from the surface into the solution. The field strength is approximately equal for all four samples because the zeta potential values are similar (∼−50 mV). The orientational ordering of the water is determined by the local surface structure (as captured by the surface susceptibility and form factor functions) as well as the interaction of the electrostatic field in the electric double layer region with the water dipoles (as captured by an effective third-order nonlinear optical response that scales linearly with the electrostatic field).[86,87] The presence of an electrostatic field therefore results in a larger overall response for DPPS/DPPG/DPPA than for DPPE and DPPC. Because the electrostatic field is approximately identical for all three charged lipids, the difference in the SHS intensity indicates a structural difference in the interfacial water order among DPPS, DPPG, and DPPA.

As illustrated in Figure 2D, the gauche defect containing (disordered) acyl chains of the three charged lipids are in close contact with the oil surface (which has disordered acyl chains that are oriented nearly parallel with respect to the interface rather than perpendicular[64]). The phospholipid headgroup has rotational freedom (Figure 2D inset) around the acyl chain axis lying in the interfacial plane. The strength of the s-CO−O−C stretching mode in the SFS spectrum depends on the distribution of this rotation. Irrespective of the headgroup rotation, however, the dipole of the s-PO_2^- mode will always be oriented along the interfacial plane and thus will be invisible in SFS. Because DPPG has a weakly visible response at ∼1073 cm^{-1} and DPPA and DPPS do not, there seems to be a difference in headgroup orientation among the three. Comparing the SHS data in Figure 2C, it is reasonable to expect that the P−N vector of the DPPS headgroup is somewhat aligned along the surface normal. This will induce additional oriented water dipoles (that can be located and H-bond between the PO_2^- and NH_3^+ groups), resulting in a stronger SHS response for DPPS compared to those for DPPA and DPPG.

The resemblance of the characteristics between the charged lipid monolayers and negatively charged surfactants[51] adsorbed to similar oil droplets suggests that the same mechanism is responsible for the low surface density in both systems. Although the molecular structures are very different, it makes sense to speculate on the origin of this phenomenon in terms of relevant interactions. At the surface of nanodroplets, charged headgroups repel each other. The ions in solution are just the counterions at (sub)-millimolar concentrations. The charged headgroups and the counterions are likely not paired.[50] Increasing the interfacial phospholipid density requires overcoming electrostatic repulsion, for example, by charge condensation of the counterions. The balance between entropic (dissociation) and enthalpic (association) forces is a delicate one that critically depends on the geometry of the interface and the ionic strength.[88] For example, for cylindrical polyelectrolytes such as DNA, the balance between the entropic and enthalpic interaction results in charge condensation under physiological conditions. Under very low ionic strength conditions such as investigated here, planar surfaces have nearly complete charge condensation, whereas small nanospheres do not.[89] For nanospheres, the oil phase contains no ions and will thus not participate in the screening of the electrostatic fields generated by the charged lipid headgroup. This is different for planar interfaces, where the charge−charge repulsion is (eventually) screened and the effective charge−charge repulsion is less. Both of these considerations result in a relatively higher repulsion at the surface of droplets than at planar interfaces.

CONCLUSIONS

We have measured the surface structure of zwitterionic (neutral) and charged phospholipids on oil nanodroplets in water and observe remarkable differences in structure. Zwitterionic phospholipids form a closely packed monolayer on oil nanodroplets, with stretched all-trans acyl chains that are almost perpendicular to the monolayer plane. For the

DOI: 10.1021/acs.langmuir.7b02896
Langmuir XXXX, XXX, XXX−XXX

zwitterionic phospholipids, the interphospholipid interaction between the P−N dipoles results in the phospholipid headgroup orienting almost parallel to the monolayer plane and forming charge pairs between the PO_2^- and $N(CH_3)_3^+$ (for PC lipids) or NH_3^+ (for PE lipids) groups. The formation of this charge pair in turn attracts neighboring phospholipids to form a closely packed phospholipid monolayer. The phospholipid-induced water ordering is limited to the interfacial region, with water dipoles oriented almost parallel to the monolayer plane on average.

In contrast, anionic phospholipids form a sparse monolayer with highly disordered acyl chains, surprisingly different from the structure reported on extended planar interfaces.[25,85] This significant difference most likely results from intermolecular interactions between phospholipid headgroups because the studied phospholipids have identical acyl chains. For the anionic phospholipids, the net negative charge in the headgroup generates a repulsive electrostatic force between phospholipid molecules. This repulsive force results in a low number density of anionic phospholipids in the monolayer. The large separation of anionic phospholipids in the monolayer increases the water contact of each phospholipid headgroup. The anionic phospholipid headgroup is oriented perpendicular to the monolayer plane by the favored H-bonding and electrostatic interactions with water. In contrast to the zwitterionic phospholipids, the anionic phospholipid-induced water ordering extends into the bulk water as a result of the electrostatic field from the net negative charge in the headgroup. These significant differences between the two types of phospholipids and the difference with respect to macroscopically extended interfaces indicate important roles of phospholipid headgroups and the length scale over which lipid monolayers are structured in the determination of properties of cellular membranes and lipid droplets. These findings can guide the design of more efficient lipid emulsion systems for drug delivery and aid our molecular-level understanding of nanoscale membranes in living systems.

■ ASSOCIATED CONTENT

Supporting Information

The Supporting Information is available free of charge on the ACS Publications website at DOI: 10.1021/acs.langmuir.7b02896.

Chemical structures of the phospholipids, additional SFS spectra of DPPE, fitting procedures for the SFS spectra, and an estimation of the acyl chain tilt angle and the tilt angle of the phosphate headgroup (PDF)

■ AUTHOR INFORMATION

Corresponding Author

*E-mail: sylvie.roke@epfl.ch.

ORCID

Yixing Chen: 0000-0001-8492-9615
Halil I. Okur: 0000-0002-2492-1168
Sylvie Roke: 0000-0002-6062-7871

Notes

The authors declare no competing financial interest.

■ ACKNOWLEDGMENTS

This work is supported by the Julia Jacobi Foundation and the European Research Council (grant 240556 and 616305).

■ REFERENCES

(1) Berg, J. M.; Tymoczko, J. L.; Stryer, L. *Biochemistry*; W. H. Freeman, 2012.
(2) Porter, C. J. H.; Trevaskis, N. L.; Charman, W. N. Lipids and Lipid-based Formulations: Optimizing the Oral Delivery of Lipophilic Drugs. *Nat. Rev. Drug Discovery* **2007**, *6*, 231.
(3) Fricker, G.; Kromp, T.; Wendel, A.; Blume, A.; Zirkel, J.; Rebmann, H.; Setzer, C.; Quinkert, R.-O.; Martin, F.; Müller-Goymann, C. Phospholipids and Lipid-Based Formulations in Oral Drug Delivery. *Pharm. Res.* **2010**, *27*, 1469.
(4) Hippalgaonkar, K.; Majumdar, S.; Kansara, V. Injectable Lipid Emulsions—Advancements, Opportunities and Challenges. *AAPS PharmSciTech* **2010**, *11*, 1526.
(5) Tauchi-Sato, K.; Ozeki, S.; Houjou, T.; Taguchi, R.; Fujimoto, T. The Surface of Lipid Droplets Is a Phospholipid Monolayer with a Unique Fatty Acid Composition. *J. Biol. Chem.* **2002**, *277*, 44507.
(6) van Meer, G.; de Kroon, A. I. P. M. Lipid Map of the Mammalian Cell. *J. Cell Sci.* **2011**, *124*, 5.
(7) van Meer, G.; Voelker, D. R.; Feigenson, G. W. Membrane Lipids: Where They Are and How They Behave. *Nat. Rev. Mol. Cell Biol.* **2008**, *9*, 112.
(8) Dowhan, W. Molecular Basis For Membrane Phospholipid Diversity: Why Are There So Many Lipids? *Annu. Rev. Biochem.* **1997**, *66*, 199.
(9) Dowhan, W. Lipids and Extracellular Materials. *Annu. Rev. Biochem.* **2014**, *83*, 45.
(10) Kaganer, V. M.; Mohwald, H.; Dutta, P. Structure and Phase Transitions in Langmuir Monolayers. *Rev. Mod. Phys.* **1999**, *71*, 779.
(11) Als-Nielsen, J.; Jacquemain, D.; Kjaer, K.; Leveiller, F.; Lahav, M.; Leiserowitz, L. Principles and Applications of Grazing Incidence X-ray and Neutron Scattering from Ordered Molecular Monolayers at the Air-water Interface. *Phys. Rep.* **1994**, *246*, 251.
(12) Kjaer, K.; Als-Nielsen, J.; Helm, C. A.; Laxhuber, L. A.; Möhwald, H. Ordering in Lipid Monolayers Studied by Synchrotron X-Ray Diffraction and Fluorescence Microscopy. *Phys. Rev. Lett.* **1987**, *58*, 2224.
(13) Brezesinski, G.; Thoma, M.; Struth, B.; Möhwald, H. Structural Changes of Monolayers at the Air/Water Interface Contacted with *n*-Alkanes. *J. Phys. Chem.* **1996**, *100*, 3126.
(14) Schalke, M.; Lösche, M. Structural Models of Lipid Surface Monolayers from X-ray and Neutron Reflectivity Measurements. *Adv. Colloid Interface Sci.* **2000**, *88*, 243.
(15) Thomas, R. K. Neutron Reflection from Liquid Interfaces. *Annu. Rev. Phys. Chem.* **2004**, *55*, 391.
(16) Krueger, S. Neutron Reflection from Interfaces with Biological and Biomimetic Materials. *Curr. Opin. Colloid Interface Sci.* **2001**, *6*, 111.
(17) McConnell, H. M. Structures and Transitions in Lipid Monolayers at the Air-Water Interface. *Annu. Rev. Phys. Chem.* **1991**, *42*, 171.
(18) Bagatolli, L. A. To See or Not to See: Lateral Organization of Biological Membranes and Fluorescence Microscopy. *Biochim. Biophys. Acta, Biomembr.* **2006**, *1758*, 1541.
(19) Crane, J. M.; Kiessling, V.; Tamm, L. K. Measuring Lipid Asymmetry in Planar Supported Bilayers by Fluorescence Interference Contrast Microscopy. *Langmuir* **2005**, *21*, 1377.
(20) Phillips, M. C.; Chapman, D. Monolayer Characteristics of Saturated 1,2-Diacyl Phosphatidylcholines (Lecithins) and Phosphatidylethanolamines at Air-Water Interface. *Biochim. Biophys. Acta, Biomembr.* **1968**, *163*, 301.
(21) Duncan, S. L.; Larson, R. G. Comparing Experimental and Simulated Pressure-Area Isotherms for DPPC. *Biophys. J.* **2008**, *94*, 2965.
(22) Roke, S.; Schins, J. M.; Müller, M.; Bonn, M. Vibrational Spectroscopic Investigation of the Phase Diagram of a Biomimetic Lipid Monolayer. *Phys. Rev. Lett.* **2003**, *90*, 128101.
(23) Sovago, M.; Vartianen, E.; Bonn, M. Observation of Buried Water Molecules in Phospholipid Membranes by Surface Sum-frequency Generation Spectroscopy. *J. Chem. Phys.* **2009**, *131*, 161107.

DOI: 10.1021/acs.langmuir.7b02896
Langmuir XXXX, XXX, XXX−XXX

(24) Ma, G.; Allen, H. C. DPPC Langmuir Monolayer at the Air-Water Interface: Probing the Tail and Head Groups by Vibrational Sum Frequency Generation Spectroscopy. *Langmuir* **2006**, *22*, 5341.
(25) Chen, X.; Hua, W.; Huang, Z.; Allen, H. C. Interfacial Water Structure Associated with Phospholipid Membranes Studied by Phase-Sensitive Vibrational Sum Frequency Generation Spectroscopy. *J. Am. Chem. Soc.* **2010**, *132*, 11336.
(26) Watry, M. R.; Tarbuck, T. L.; Richmond, G. L. Vibrational Sum-Frequency Studies of a Series of Phospholipid Monolayers and the Associated Water Structure at the Vapor/Water Interface. *J. Phys. Chem. B* **2003**, *107*, 512.
(27) Johnson, C. M.; Baldelli, S. Vibrational Sum Frequency Spectroscopy Studies of the Influence of Solutes and Phospholipids at Vapor/Water Interfaces Relevant to Biological and Environmental Systems. *Chem. Rev.* **2014**, *114*, 8416.
(28) Mondal, J. A.; Nihonyanagi, S.; Yamaguchi, S.; Tahara, T. Three Distinct Water Structures at a Zwitterionic Lipid/Water Interface Revealed by Heterodyne-Detected Vibrational Sum Frequency Generation. *J. Am. Chem. Soc.* **2012**, *134*, 7842.
(29) Backus, E. H. G.; Bonn, D.; Cantin, S.; Roke, S.; Bonn, M. Laser-Heating-Induced Displacement of Surfactants on the Water Surface. *J. Phys. Chem. B* **2012**, *116*, 2703.
(30) Walker, R. A.; Conboy, J. C.; Richmond, G. L. Molecular Structure and Ordering of Phospholipids at a Liquid-liquid Interface. *Langmuir* **1997**, *13*, 3070.
(31) Walker, R. A.; Gruetzmacher, J. A.; Richmond, G. L. Phosphatidylcholine Monolayer Structure at a Liquid-liquid Interface. *J. Am. Chem. Soc.* **1998**, *120*, 6991.
(32) Liljeblad, J. F. D.; Bulone, V.; Rutland, M. W.; Johnson, C. M. Supported Phospholipid Monolayers. The Molecular Structure Investigated by Vibrational Sum Frequency Spectroscopy. *J. Phys. Chem. C* **2011**, *115*, 10617.
(33) Liu, W.; Wang, Z.; Fu, L.; Leblanc, R. M.; Yan, E. C. Y. Lipid Compositions Modulate Fluidity and Stability of Bilayers: Characterization by Surface Pressure and Sum Frequency Generation Spectroscopy. *Langmuir* **2013**, *29*, 15022.
(34) Kim, J.; Kim, G.; Cremer, P. S. Investigations of Water Structure at the Solid/Liquid Interface in the Presence of Supported Lipid Bilayers by Vibrational Sum Frequency Spectroscopy. *Langmuir* **2001**, *17*, 7255.
(35) Liu, J.; Conboy, J. C. Structure of a Gel Phase Lipid Bilayer Prepared by the Langmuir-Blodgett/Langmuir-Schaefer Method Characterized by Sum-frequency Vibrational Spectroscopy. *Langmuir* **2005**, *21*, 9091.
(36) Liu, J.; Conboy, J. C. Direct Measurement of the Transbilayer Movement of Phospholipids by Sum-frequency Vibrational Spectroscopy. *J. Am. Chem. Soc.* **2004**, *126*, 8376.
(37) Dominguez, H.; Smondyrev, A. M.; Berkowitz, M. L. Computer Simulations of Phosphatidylcholine Monolayers at Air/Water and CCl4/Water Interfaces. *J. Phys. Chem. B* **1999**, *103*, 9582.
(38) Shinoda, W.; DeVane, R.; Klein, M. L. Zwitterionic Lipid Assemblies: Molecular Dynamics Studies of Monolayers, Bilayers, and Vesicles Using a New Coarse Grain Force Field. *J. Phys. Chem. B* **2010**, *114*, 6836.
(39) Bennett, W. F. D.; Tieleman, D. P. Computer Simulations of Lipid Membrane Domains. *Biochim. Biophys. Acta, Biomembr.* **2013**, *1828*, 1765.
(40) Berkowitz, M. L.; Bostick, D. L.; Pandit, S. Aqueous Solutions Next to Phospholipid Membrane Surfaces: Insights from Simulations. *Chem. Rev.* **2006**, *106*, 1527.
(41) Chen, Y.; Jena, K. C.; Lütgebaucks, C.; Okur, H. I.; Roke, S. Three Dimensional Nano "Langmuir Trough" for Lipid Studies. *Nano Lett.* **2015**, *15*, 5558.
(42) Okur, H. I.; Chen, Y.; Smolentsev, N.; Zdrali, E.; Roke, S. Interfacial Structure and Hydration of 3D Lipid Monolayers in Aqueous Solution. *J. Phys. Chem. B* **2017**, *121*, 2808.
(43) Liljeblad, J. F. D.; Bulone, V.; Tyrode, E.; Rutland, M. W.; Johnson, C. M. Phospholipid Monolayers Probed by Vibrational Sum Frequency Spectroscopy: Instability of Unsaturated Phospholipids. *Biophys. J.* **2010**, *98*, L50.
(44) Delcerro, C.; Jameson, G. J. The Behavior of Pentane, Hexane, and Heptane on Water. *J. Colloid Interface Sci.* **1980**, *78*, 362.
(45) Goebel, A. K.; Lunkenheimer, K. Interfacial Tension of the Water/n-Alkane Interface. *Langmuir* **1997**, *13*, 369.
(46) Jena, K. C.; Scheu, R.; Roke, S. Surface Impurities Are Not Responsible For the Charge on the Oil/Water Interface: A Comment. *Angew. Chem., Int. Ed.* **2012**, *51*, 12938.
(47) Wang, H.; Yan, E. C. Y.; Borguet, E.; Eisenthal, K. B. Second harmonic generation from the surface of centrosymmetric particles in bulk solution. *Chem. Phys. Lett.* **1996**, *259*, 15.
(48) Yan, E. C. Y.; Eisenthal, K. B. Effect of Cholesterol on Molecular Transport of Organic Cations Across Liposome Bilayers Probed by Second Harmonic Generation. *Biophys. J.* **2000**, *79*, 898.
(49) Liu, Y.; Yan, E. C. Y.; Eisenthal, K. B. Effects of Bilayer Surface Charge Density on Molecular Adsorption and Transport Across Liposome Bilayers. *Biophys. J.* **2001**, *80*, 1004.
(50) Scheu, R.; Chen, Y.; Subinya, M.; Roke, S. Stern Layer Formation Induced by Hydrophobic Interactions: A Molecular Level Study. *J. Am. Chem. Soc.* **2013**, *135*, 19330.
(51) Scheu, R.; Chen, Y.; de Aguiar, H. B.; Rankin, B. M.; Ben-Amotz, D.; Roke, S. Specific Ion Effects in Amphiphile Hydration and Interface Stabilization. *J. Am. Chem. Soc.* **2014**, *136*, 2040.
(52) Lütgebaucks, C.; Gonella, G.; Roke, S. Optical Label-free and Model-free Probe of the Surface Potential of Nanoscale and Microscopic Objects in Aqueous Solution. *Phys. Rev. B: Condens. Matter Mater. Phys.* **2016**, *94*, 195410.
(53) Lütgebaucks, C.; Macias-Romero, C.; Roke, S. Characterization of the Interface of Binary Mixed DOPC:DOPS Liposomes in Water: The Impact of Charge Condensation. *J. Chem. Phys.* **2017**, *146*, 044701.
(54) Scheu, R.; Rankin, B. M.; Chen, Y.; Jena, K. C.; Ben-Amotz, D.; Roke, S. Charge Asymmetry at Aqueous Hydrophobic Interfaces and Hydration Shells. *Angew. Chem., Int. Ed.* **2014**, *53*, 9560.
(55) de Aguiar, H. B.; de Beer, A. G. F.; Strader, M. L.; Roke, S. The Interfacial Tension of Nanoscopic Oil Droplets in Water Is Hardly Affected by SDS Surfactant. *J. Am. Chem. Soc.* **2010**, *132*, 2122.
(56) Smolentsev, N.; Smit, W. J.; Bakker, H. J.; Roke, S. The Interfacial Structure of Water Droplets in a Hydrophobic Liquid. *Nat. Commun.* **2017**, *8*, 15548.
(57) Gomopoulos, N.; Lütgebaucks, C.; Sun, Q. C.; Macias-Romero, C.; Roke, S. Label-free Second Harmonic and Hyper Rayleigh Scattering with High Efficiency. *Opt. Express* **2013**, *21*, 815.
(58) de Aguiar, H. B.; Samson, J. S.; Roke, S. Probing Nanoscopic Droplet Interfaces in Aqueous Solution with Vibrational Sum-frequency Scattering: A Study of the Effects of Path Length, Droplet Density and Pulse Energy. *Chem. Phys. Lett.* **2011**, *512*, 76.
(59) Roke, S.; Gonella, G. Nonlinear Light Scattering and Spectroscopy of Particles and Droplets in Liquids. *Annu. Rev. Phys. Chem.* **2012**, *63*, 353.
(60) Guyot-Sionnest, P.; Hunt, J. H.; Shen, Y. R. Sum-frequency Vibrational Spectroscopy of a Langmuir Film: Study of Molecular Orientation of a Two-dimensional System. *Phys. Rev. Lett.* **1987**, *59*, 1597.
(61) Esenturk, O.; Walker, R. A. Surface Vibrational Structure at Alkane Liquid/Vapor Interfaces. *J. Chem. Phys.* **2006**, *125*, 174701.
(62) Tyrode, E.; Hedberg, J. A Comparative Study of the CD and CH Stretching Spectral Regions of Typical Surfactants Systems Using VSFS: Orientation Analysis of the Terminal CH3 and CD3 Groups. *J. Phys. Chem. C* **2012**, *116*, 1080.
(63) Smolentsev, N.; Lütgebaucks, C.; Okur, H. I.; de Beer, A. G. F.; Roke, S. Intermolecular Headgroup Interaction and Hydration as Driving Forces for Lipid Transmembrane Asymmetry. *J. Am. Chem. Soc.* **2016**, *138*, 4053.
(64) de Aguiar, H. B.; Strader, M. L.; de Beer, A. G. F.; Roke, S. Surface Structure of SDS Surfactant and Oil at the Oil-in-water Droplet Liquid/Liquid Interface: A Manifestation of a Non-equilibrium Surface State. *J. Phys. Chem. B* **2011**, *115*, 2970.

DOI: 10.1021/acs.langmuir.7b02896
Langmuir XXXX, XXX, XXX−XXX

(65) Chen, Y.; Okur, H. I.; Gomopoulos, N.; Macias-Romero, C.; Cremer, P. S.; Petersen, P. B.; Tocci, G.; Wilkins, D. M.; Liang, C.; Ceriotti, M.; Roke, S. Electrolytes Induce Long-range Orientational Order and Free Energy Changes in the H-bond Network of Bulk Water. *Sci. Adv.* **2016**, *2*, e1501891.
(66) Chen, X.; Allen, H. C. Interactions of Dimethylsulfoxide with a Dipalmitoylphosphatidylcholine Monolayer Studied by Vibrational Sum Frequency Generation. *J. Phys. Chem. A* **2009**, *113*, 12655.
(67) Hauser, H.; Pascher, I.; Pearson, R. H.; Sundell, S. Preferred Conformation and Molecular Packing of Phosphatidylethanolamine and Phosphatidylcholine. *Biochim. Biophys. Acta, Rev. Biomembr.* **1981**, *650*, 21.
(68) Wei, F.; Xiong, W.; Li, W.; Lu, W.; Allen, H. C.; Zheng, W. Assembly and Relaxation Behaviours of Phosphatidylethanolamine Monolayers Investigated by Polarization and Frequency Resolved SFG-VS. *Phys. Chem. Chem. Phys.* **2015**, *17*, 25114.
(69) Pohle, W.; Selle, C.; Fritzsche, H.; Bohl, M. Comparative FTIR Spectroscopic Study upon the Hydration of Lecithins and Cephalins. *J. Mol. Struct.* **1997**, *408−409*, 273.
(70) Casal, H. L.; Mantsch, H. H.; Paltauf, F.; Hauser, H. Infrared and 31P-NMR Studies of the Effect of Li+ and Ca2+ on Phosphatidylserines. *Biochim. Biophys. Acta, Lipids Lipid Metab.* **1987**, *919*, 275.
(71) Casillas-Ituarte, N.; Chen, X.; Castada, H.; Allen, H. C. Na+ and Ca2+ Effect on the Hydration and Orientation of the Phosphate Group of DPPC at Air-Water and Air-Hydrated Silica Interfaces. *J. Phys. Chem. B* **2010**, *114*, 9485.
(72) Raman, P.; Cherezov, V.; Caffrey, M. The Membrane Protein Data Bank. *Cell. Mol. Life Sci.* **2006**, *63*, 36.
(73) Cordomí, A.; Edholm, O.; Perez, J. J. Effect of Ions on a Dipalmitoyl Phosphatidylcholine Bilayer. A Molecular Dynamics Simulation Study. *J. Phys. Chem. B* **2008**, *112*, 1397.
(74) Vácha, R.; Siu, S. W. I.; Petrov, M.; Böckmann, R. A.; Barucha-Kraszewska, J.; Jurkiewicz, P.; Hof, M.; Berkowitz, M. L.; Jungwirth, P. Effects of Alkali Cations and Halide Anions on the DOPC Lipid Membrane. *J. Phys. Chem. A* **2009**, *113*, 7235.
(75) Browning, J. L. Motions and Interactions of Phospholipid Head Groups at the Membrane Surface. 2. Head Groups with Hydroxyl Groups. *Biochemistry* **1981**, *20*, 7133.
(76) Seelig, J. 31P Nuclear Magnetic Resonance and the Head Group Structure of Phospholipids in Membranes. *Biochim. Biophys. Acta, Rev. Biomembr.* **1978**, *515*, 105.
(77) Vácha, R.; Rick, S. W.; Jungwirth, P.; de Beer, A. G. F.; de Aguiar, H. B.; Samson, J. S.; Roke, S. The Orientation and Charge of Water at the Hydrophobic Oil Droplet-Water Interface. *J. Am. Chem. Soc.* **2011**, *133*, 10204.
(78) Agmon, N.; Bakker, H. J.; Campen, R. K.; Henchman, R. H.; Pohl, P.; Roke, S.; Thämer, M.; Hassanali, A. Protons and Hydroxide Ions in Aqueous Systems. *Chem. Rev.* **2016**, *116*, 7642.
(79) Eisenthal, K. B. Liquid Interfaces Probed by Second-Harmonic and Sum-Frequency Spectroscopy. *Chem. Rev.* **1996**, *96*, 1343.
(80) Pasenkiewicz-Gierula, M.; Takaoka, Y.; Miyagawa, H.; Kitamura, K.; Kusumi, A. Charge Pairing of Headgroups in Phosphatidylcholine Membranes: A Molecular Dynamics Simulation Study. *Biophys. J.* **1999**, *76*, 1228.
(81) Milhaud, J. New Insights into Water-phospholipid Model Membrane Interactions. *Biochim. Biophys. Acta, Biomembr.* **2004**, *1663*, 19.
(82) Zhou, F.; Schulten, K. Molecular-Dynamics Study of a Membrane Water Interface. *J. Phys. Chem.* **1995**, *99*, 2194.
(83) Damodaran, K. V.; Merz, K. M. Head Group Water Interactions in Lipid Bilayers - a Comparison between DMPC-Based and DLPE-Based Lipid Bilayers. *Langmuir* **1993**, *9*, 1179.
(84) Zhang, Y. P.; Lewis, R. N. A. H.; Mcelhaney, R. N.; Ryan, R. O. Calorimetric and Spectroscopic Studies of the Interaction of Manduca-Sexta Apolipophorin-Iii with Zwitterionic, Anionic and Nonionic Lipids. *Biochemistry* **1993**, *32*, 3942.
(85) Mondal, J.; Nihonyanagi, S.; Yamaguchi, S.; Tahara, T. Structure and Orientation of Water at Charged Lipid Monolayer/Water Interfaces Probed by Heterodyne-Detected Vibrational Sum Frequency Generation Spectroscopy. *J. Am. Chem. Soc.* **2010**, *132*, 10656.
(86) de Beer, A. G. F.; Campen, R. K.; Roke, S. Separating Surface Structure and Surface Charge with Second-harmonic and Sum-frequency Scattering. *Phys. Rev. B: Condens. Matter Mater. Phys.* **2010**, *82*, 235431.
(87) Gonella, G.; Lütgebaucks, C.; de Beer, A. G. F.; Roke, S. Second Harmonic and Sum-Frequency Generation from Aqueous Interfaces Is Modulated by Interference. *J. Phys. Chem. C* **2016**, *120*, 9165.
(88) Manning, G. S. Counterion Condensation on Charged Spheres, Cylinders, and Planes. *J. Phys. Chem. B* **2007**, *111*, 8554.
(89) Zimm, B. H.; Bret, M. L. Counter-Ion Condensation and System Dimensionality. *J. Biomol. Struct. Dyn.* **1983**, *1*, 461.

DOI: 10.1021/acs.langmuir.7b02896
Langmuir XXXX, XXX, XXX−XXX